Lab on a Chip

Accepted Manuscript

ROYAL SOCIETY OF CHEMISTRY

www.rsc.org/loc

This paper describes the ability for dielectrophoresis to enrich and recover antibiotic-treated mycobacteria, based on physico-chemical properties of their membranes.

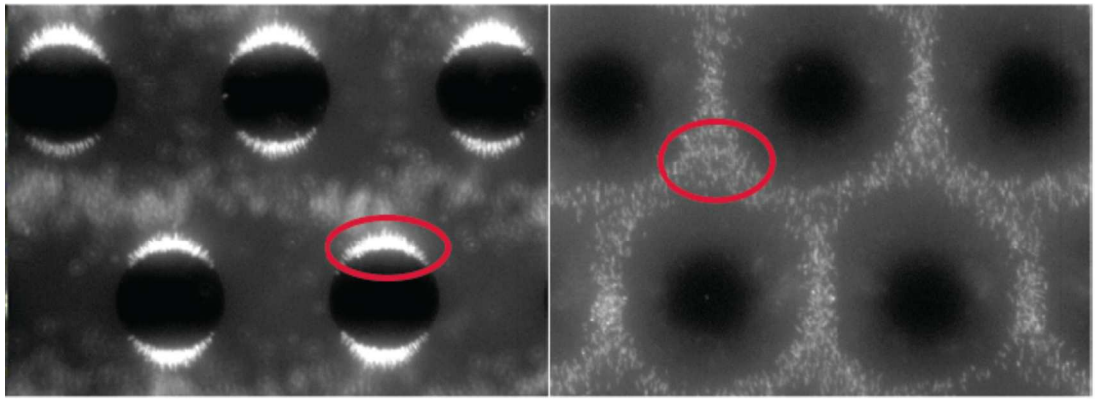

Dielectrophoresis-based purification of antibiotic-treated bacterial subpopulations

Meltem Elitas[1,3], Rodrigo Martinez-Duarte[2,4*], Neeraj Dhar[1], John D. McKinney[1], and Philippe Renaud[2]

[1]School of Life Sciences, École Polytechnique Fédérale de Lausanne (EPFL), 1015 Lausanne, Switzerland

[2]Laboratory of Microsystems, École Polytechnique Fédérale de Lausanne (EPFL), 1015 Lausanne, Switzerland

[3]Current Address: Department of Biomedical Engineering, Yale University, New Haven, CT 06520 USA

[4]Current Address: Department of Mechanical Engineering, Clemson University, Clemson, SC 29634 USA

*Corresponding author: rodrigm@clemson.edu

Keywords: 3D carbon-electrode dielectrophoresis, persistence, persisters, antibiotics, isoniazid, phenotypic tolerance, cell fractionation.

Abstract

Persistence of bacteria during antibiotic therapy is a widespread phenomenon, of particular importance in refractory mycobacterial infections such as leprosy and tuberculosis. Persistence is characterized by the phenotypic tolerance of a subpopulation of bacterial cells to antibiotics. Characterization of these "persister" cells is often difficult due to the transient, non-heritable nature of the phenotype and due to the presence of contaminating material from non-persisting cells, which usually comprise the larger fraction. In this study, we use 3D carbon-electrode arrays for dielectrophoresis-based separation of intact cells from damaged cells, revealed by differential staining with propidium iodide, and we use this procedure to purify intact cells from cultures of *Mycobacterium smegmatis* treated with isoniazid, a frontline anti-tuberculosis drug. The method presented in this study could be used for rapid label-free enrichment of intact persister cells from antibiotic-treated cultures while preserving the metastable persister phenotype. This approach would facilitate the downstream analysis of low-frequency subpopulations of cells using conventional omics techniques, such as transcriptomic and proteomic analysis.

1. Introduction

Bacterial persistence, first described by Bigger in 1944 [1], has been observed in many different bacterial species exposed to different classes of antimicrobials. Bacterial persistence is a clinically important problem, as it is thought to be responsible for treatment failures, post-therapy relapses, and lengthy treatment regimens in diseases such as leprosy and tuberculosis. Despite this, there have not been many studies carried out to characterize these persisters or to understand the mechanism of persistence, chiefly due to the following reasons. First, the fraction of persister cells is often very small (10^{-3} to 10^{-6} or lower), which complicates their analysis within mixed populations comprising persister (minority) and non-persister (majority) subpopulations. Second, the persister phenotype is not mediated through genetic changes and therefore is non-heritable. Instead, the phenotype is transient, usually lasting only as long as the drug remains in the environment. This makes it difficult to purify or isolate the tolerant subpopulations for further analysis. Third, since the persister fraction is usually a small fraction of the total population, analysis of this subpopulation is often confounded by contaminating

signals from the majority non-persister dead cells or cell debris. Besides making it difficult to treat infections, the persistence phenomenon may also increase the probability of emergence of genetic resistance, thus contributing to the short lifespan of antibiotics after they reach the market. Therefore, there is a pressing need for new experimental tools to address the phenomenon of bacterial persistence. A better characterization of the persister sub-population could enable the design of new drugs that target the persister population and help in reducing the duration of treatment of recalcitrant infections [2], [3].

At the single-cell level, bacterial populations exhibit substantial heterogeneity in their response to antibiotics. While a bactericidal antibiotic typically kills the majority of the population, subpopulations of long-term surviving bacteria are usually present. A fraction of the surviving subpopulation may resume growth immediately after drug washout, and this subpopulation can be scored by conventional methods such as plating for colony forming units (CFU) on solid medium. However, there may be other subpopulations that also persist during drug exposure but which are usually overlooked, such as cells that enter a "non-growing but metabolically active" (NGMA) state, which are not able to form colonies and are therefore not detected in CFU assays [4]. NGMA cells, which may comprise a significant fraction of the surviving population, remain physically intact and exclude so-called "live/dead" stains such as propidium iodide (PI), which preferentially stains cells with damaged cell walls. This cryptic cell population may retain the potential to resume growth under appropriate culture conditions. Finally, among antibiotic-treated populations there are also cells that appear to be physically intact in phase-contrast images yet are PI-positive in fluorescence images, indicating that their cell envelopes have been damaged. By convention, PI-positive cells are routinely scored as "dead", although that assumption has recently been challenged [5]. New tools are needed to fractionate antibiotic-treated populations in order to purify phenotypically distinct subpopulations without altering their phenotypes. Purification would facilitate the characterization of these subpopulations using conventional 'omics-based approaches [6], [7]. While fluorescence-activated cell sorting (FACS) is the most common enrichment technique and provides high-throughput fractionation of cell populations, this technique requires cells to be differentially labeled, which could potentially change the phenotype of the organism.

Dielectrophoresis (DEP) is a technique in which a dielectric particle, when placed in a non-uniform electric field, experiences a propulsive force that can be positive (movement towards

regions of high field strength) or negative (movement towards regions of low field strength). This property of dielectric particles has been used for the manipulation, separation, and concentration of different bioparticles [8], including bacterial cells [9], [10], [11], infected cells from blood [11], viruses [12], DNA [13], RNA [14], and proteins [15], [16], [17]. An important advantage of DEP-based approaches is that they do not require pre-labelling of the cells, because the separation relies instead on innate physical properties (dielectric properties) of the particle itself. Changes to the physical features, such as surface morphology or membrane integrity, impart a differential dielectric force on the cell, allowing separation in a non-uniform electric field. Advances in DEP and in microfabrication techniques have allowed different kinds of electrode geometries to be implemented in the quest for a robust, low-cost, high-throughput separation system [18], [19]. In the present study, we use carbon 3D electrodes to induce the DEP force, and we use this setup for the DEP-based fractionation of subpopulations of mycobacteria following exposure to isoniazid (INH), a frontline anti-tuberculosis drug. INH-mediated killing follows biphasic kinetics, in which a rapid "killing" phase is followed by a prolonged "persistence" phase due to survival of a subpopulation of INH-tolerant persister cells [20]. Using the non-pathogenic strain *Mycobacterium smegmatis*, we establish protocols for DEP-based purification of INH-treated subpopulations, and in a proof-of-concept study we demonstrate label-free isolation and enrichment of persisters in sufficient numbers for downstream analysis using conventional methods such as proteomic and transcriptomic analysis.

2. Materials and Methods

2.1 Dielectrophoresis

Although the focus of this paper is not a theoretical treatment of DEP, we provide the basic equations on the effect of positive and negative DEP; further details on the theory behind DEP can be found elsewhere [21], [22]. The DEP force induced on a particle depends on the magnitude and non-uniformity of an externally applied electric field, as well as the relation between the physical and electrical parameters, such as conductivity and permeability, of the surrounding medium and the targeted cell, as described in Equation 1.

$$F_{DEP} = 2\pi\varepsilon_m r^3 \mathrm{Re}[f_{CM}]\nabla E_{rms}^2 \quad (1)$$

where r is the radius of the cell, E_{rms} the root mean square of the electric field (which is related to the geometry of the electrodes polarizing the sample), ε_m the permittivity of the medium,

$\mathrm{Re}[f_{CM}]$ the real part of the Clausius-Mossotti factor (f_{CM}) defined as

$$\mathrm{Re}[f_{CM}] = \frac{\varepsilon_p^* - \varepsilon_m^*}{\varepsilon_p^* + 2\varepsilon_m^*} \quad (2)$$

with ε_p^* being the complex permittivity of the particle, and ε_m^* that of the medium. Complex permittivity ε^* is given by

$$\varepsilon^* = \varepsilon - \frac{j\sigma}{2\pi f} \quad (3)$$

and depends on the permittivity (ε) and conductivity (σ) of the cell or the medium and the frequency f of the applied electric field. j represents the imaginary number $\sqrt{-1}$. $\mathrm{Re}[f_{CM}]$ can vary from -0.5 to 1. The positive sign of $\mathrm{Re}[f_{CM}]$ denotes the induction of a DEP force that causes cells to migrate towards regions of high field strength, which is designated positive dielectrophoresis (pDEP). Negative values of $\mathrm{Re}[f_{CM}]$ denote the opposite behavior, cells moving toward regions of low or no field strength, and accordingly is designated negative dielectrophoresis (nDEP). Whether a cell displays pDEP or nDEP depends on polarizability of the cell with respect to its surrounding medium.

2.2 Low Conductive DEP Buffer Preparation

The low conductive buffer for DEP was prepared by diluting 10 ml of phosphate-buffered saline (PBS, Gibco) with 390 ml of double-distilled water, which was further supplemented with 10 ml of 10% Tween-80 (Sigma-Aldrich) and 30 mg of bovine serum albumin (BSA). The conductivity of the final suspension was 500 μS/cm, as measured by a conductivity meter (Cole-Parmer Instruments). Viability of bacteria in this DEP buffer was compared to viability in growth medium using culture assays. Viability curves of *M. smegmatis* in both growth medium and DEP buffer were similar up to 4 hours (data not shown).

2.3 Sample Preparation and Fluorescent Staining

We used *M. smegmatis* expressing a fluorescent reporter or we stained the bacteria with different fluorescent markers in order to facilitate their visualization; however, it is important to note that such staining is not required for DEP, which can be carried out with unstained samples. In fact, the ultimate goal of this work was to implement a DEP tool to purify a viable subpopulation of cells in a "color-blind" assay. *M. smegmatis* cells expressing GFP constitutively from an integrated plasmid were grown overnight, to an $OD_{600\ nm}$ of 0.5 (Thermo scientific, Biomates), in

standard Middlebrook 7H9 medium (BD/Difco) containing 0.5% albumin, 0.085% NaCl, 0.2% glucose, 0.05% Tween-80, and 0.5% glycerol at 37˚C with shaking at 200 rpm. The overnight culture was diluted to an $OD_{600\ nm}$ of 0.05 using complete Middlebrook 7H9 medium and then exposed to INH (50 µg/ml, Sigma-Aldrich) for 24 hours. After antibiotic treatment, the cell suspension was prepared by collecting antibiotic-treated cells by centrifugation (~ 900 x g (rcf), 10 min), followed by four washes (~ 10,000 x g, 2 min in DEP buffer) and resuspension in DEP buffer (500 µS/cm) (Fig. 1). Propidium iodide (PI) was then added at a final concentration of 1 µg/ml to stain cells whose cell wall permeability barrier was compromised during antibiotic treatment. This allowed for the observation of both "intact" cells (PI-negative) and "damaged" cells (PI-positive) by fluorescence microscopy by simply switching filters during experiments. Finally, the cell suspension was passed through a 0.5 µm filter (Millex-SV) to remove any cell agglomerates.

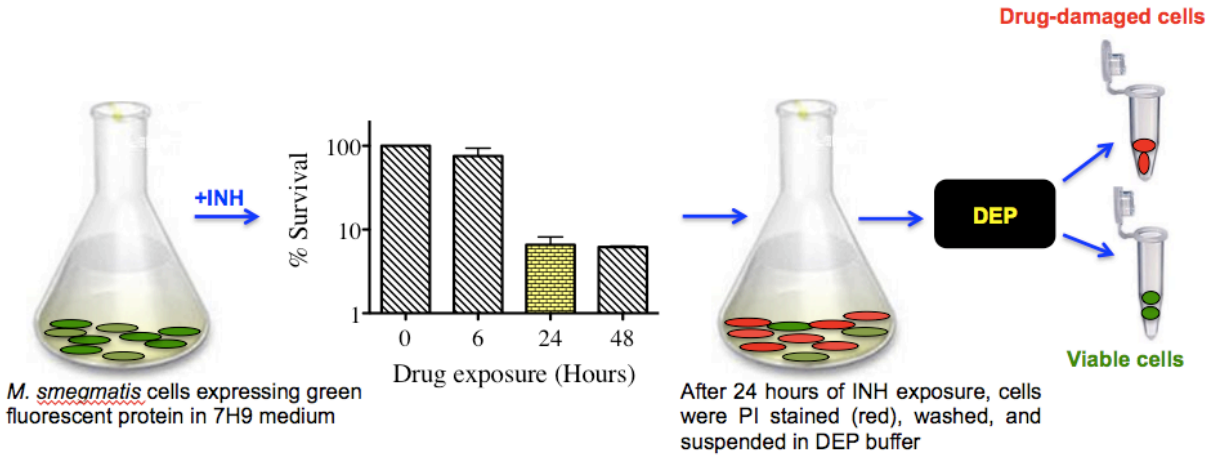

Figure 1. Schematic of dielectrophoretic separation of intact cells and drug-damaged cells after INH treatment. Cultures of *M. smegmatis* cells expressing green fluorescent protein (GFP) were grown to mid-log phase (OD_{600} ~ 0.5) in 7H9 medium. Cells were exposed to INH for 24 hours and stained with PI (red) to distinguish intact cells (GFP-positive, PI-negative) from drug-damaged cells (GFP-positive, PI-positive), then washed and resuspended in DEP Buffer (500 µS/cm). The cell suspension was passed through a syringe filter (5 µm pore size) to remove clumps. The clarifed sample was introduced into the DEP system and intact cells were enriched by pDEP for downstream analysis.

2.4 CarbonDEP Device Fabrication

In the 3D-carbonDEP device, carbon electrodes are used to induce DEP as demonstrated previously [18], [23], [24,25], [26]. Glass-like carbon electrodes are manufactured on a transparent fused silica substrate by the pyrolysis of photo-patterned epoxy-based resists in a process described previously [18]. The electrode array, of up to 2,730 posts, features an intercalated geometry as shown in Fig. 2. Electrode dimensions in the devices used here are 50 μm diameter by 100 μm height. Spacing between electrodes is 58 μm in both horizontal and vertical axes. A microfluidics channel, previously fabricated in double-sided pressure-sensitive adhesive and polycarbonate, is then manually positioned around the electrode array. Channel cross-section is 2 mm width by 100 μm height. Length of channel is 3 cm. The electrical configuration to polarize the electrodes is also shown in Fig. 2. CarbonDEP devices were washed before each experiment using a stringent washing procedure with soap and water.

2.5 Analysis

Images were captured using a Leica DMI3000B inverted fluorescent microscope with 40X objective. All frames were acquired during the experiment and later integrated into time-lapse movies, using ImageJ, to study the behavior of the bacteria under different conditions.

2.6 Assay and Data Collection

We performed two sequential 3D-carbonDEP assays. First, we analyzed an INH-treated *M. smegmatis* cell suspension to assess the behavior of cell subpopulations at different frequencies and to identify an optimal frequency for separation of intact (PI-negative) and damaged (PI-positive) cells. Second, we carried out a preparative-scale flow-through separation to enrich intact cells from a drug-treated suspension.

i. Dielectrophoretic Characterization Assay

First we characterized INH-treated *M. smegmatis* suspensions to determine the optimal frequency at which intact cells and drug-damaged cells responded differently to the applied electric field. The 3D-carbonDEP device was mounted on the stage of an inverted microscope. The cell suspension was pipetted into the 3D-carbonDEP device through the inlet port. No flow was established in the system and cells were stationary before polarizing the electrode array.

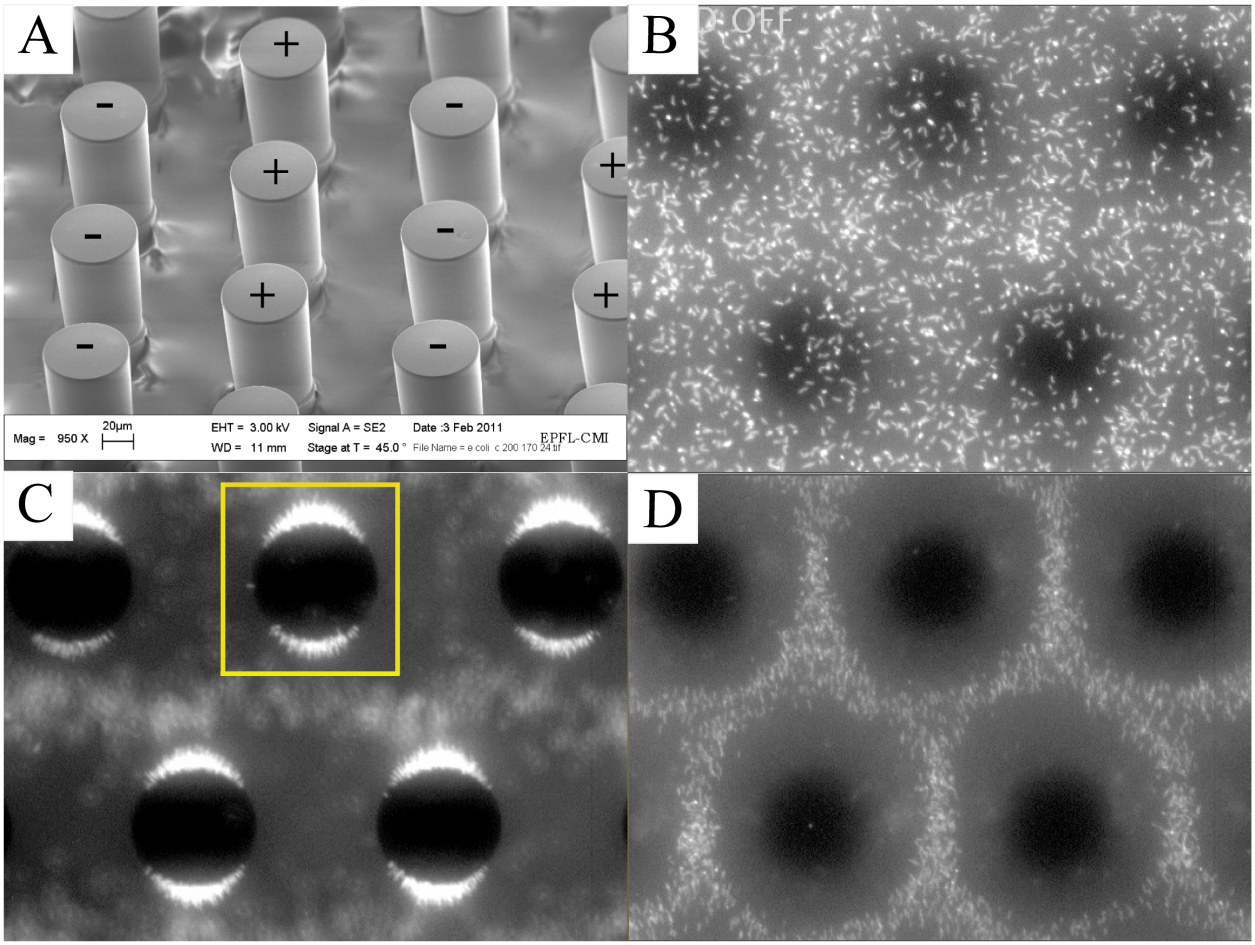

Figure 2. 3D carbon-electrode array and DEP-based analysis of INH-treated bacteria. A) Glass-like carbon electrodes on a transparent fused silica substrate. The electrical configuration is indicated. Electrode dimensions are 50 µm diameter by 100 µm height. Spacing between electrodes is 58 µm in both horizontal and vertical axes. Channel cross-section is 2 mm width by 100 µm height. Length of channel is 3 cm. There is no fluid flow in these experiments. **B)** The electric field is off. *M. smegmatis* cells appear white due to GFP expression. Carbon electrodes appear black. **C)** pDEP behavior with 20 Vpp and 7 MHz electric field signal. The cells accumulate at regions of high electric field strength. The rectangular frame indicates the area within which the fluorescence intensity measurements were performed and normalized (see Figure 3). **D)** nDEP behavior with 20 Vpp and 100 kHz electrical field signal. The cells are repelled by electrodes and accumulate at regions of weak electric field strength.

The electric field was then turned on to apply a sinusoidal signal featuring a magnitude of 20 Vpp ($V_{peak\text{-}peak}$) and a specific frequency within the range of 100 kHz to 15 MHz using an Aim-TTI TG2000 20 MHz DDS function generator (HP8657A, Agilent, Santa Clara, CA). Time-lapse movies were made to monitor the behavior of the bacterial cells at each tested frequency (examples in Supplementary Information Movies 1 and 2). In order to obtain quantitative data, three independent experiments with five replicates for a given frequency were analyzed by measuring the total intensity in a defined rectangular region, Fig. 3. Each analysis was performed by measuring the total intensity under the rectangular area and the total fluorescence intensity of the region was taken to correspond to the number of trapped cells around the electrodes. The resulting intensity versus frequency data for each experiment were plotted to derive mean intensity and standard error for characterization of INH-treated *M. smegmatis* populations.

ii. Dielectrophoretic Separation Assay

For the flow-through cell separation assay, cells were prepared as described above (Fig. 1). First, the prepared cell culture was loaded into the 3D-carbonDEP system using a syringe. The total volume of the system was 70 µl; inlet and outlet tubing carried 30 µl while the electrode array held 10 µl. After filling the complete fluidic system with the bacteria sample, DEP buffer (σ = 500 µS/cm) was pumped at a constant rate of 2 µl/min (Harvard Apparatus PHD2000 Programmable Syringe Pump). Simultaneous with the start of such flow, the field was turned on with 20 Vpp and 7 MHz to start trapping intact cells. Therefore, only a bacteria-containing plug of 40 µl (30 µl in the entrance tubing + 10 µl in the chip) was subjected to DEP. The 30 µl volume contained in the exit tubing at the beginning of the experiment was not exposed to the electric field but was still recovered and analyzed as the control fraction. The electric field remained ON for 50 minutes, during which 40 µl of sample plus 60 µl of clean DEP buffer were subjected to DEP. The purpose was to trap all antibiotic-treated intact cells on the electrodes and later do a thorough wash using clean DEP buffer. Drug-damaged cells were repelled from the electrodes and eluted to the outlet. At minute 50, the electric field was turned OFF and all bacteria previously trapped in the electrode array were released and eluted out of the channel. Flow was stopped 25 minutes later for a total experiment time of 75 minutes. A total of 15 fractions of volume 10 µl were collected throughout the experiment and the recovered serial

fractions were analyzed by flow cytometry. The aliquots (10 µl) of each collected fraction from 3D-carbonDEP assay were diluted with 200 µl DEP buffer (500 µS/cm). Unstained non-fluorescent suspensions of wild-type *M. smegmatis* were prepared in the same manner as antibiotic-treated cultures to be included as controls. All samples were then analyzed using flow cytometry (BD Accuri C6) in conjunction with CFlow software to obtain the percentage of "intact" cells (GFP-positive, PI-negative) and "drug-damaged" cells (GFP-positive, PI-positive) in each fraction.

3. Results

3.1 Dielectrophoretic characterization of INH-treated *M. smegmatis* via 3D-carbonDEP

The DEP procedure requires low conductive buffers to induce a positive DEP (pDEP) force resulting in trapping of cells on the electrodes. As per equation 2, when the suspending medium is more polarizable than the cell, negative DEP (nDEP) will result. Extraction of bacteria from the microfluidic flow requires a strong pDEP force, and thus a medium featuring polarizability much less than that of the targeted bacteria is desirable. Besides low conductivity, the suspending medium must also feature optimal values of pH and osmolarity to maintain viability of the cell population throughout the experiment. Therefore, we first optimized the conductive buffer and subsequently used it to determine the frequency-dependent behavior of individual cells in an antibiotic-treated population. The general scheme of the procedure is illustrated in Fig. 1. Cultures of *M. smegmatis* were exposed to 10-fold the minimal inhibitory concentration (MIC) of INH for 24 hours, following which they were washed and resuspended in the DEP conductive buffer. This cell suspension was then loaded into the 3D-carbon electrode array DEP device (Fig. 2A, B) as per the methodology presented above. Electric fields with frequencies between 1 and 10 MHz induce a clear pDEP behavior on the intact (PI-negative) *M. smegmatis* cells, thus attracting them to the surfaces of the electrodes (Fig. 2C, Supplementary Movie 1/pDEP). The use of frequencies less than 500 kHz leads to strong nDEP forces, as a result of which the bacteria are repelled by the electrodes and they accumulate in the weak electric field regions (Fig. 2D, Supplementary Movie 2/nDEP). For the purpose of optimizing conditions and for aiding visualization of cells in microscopic images, we used an *M. smegmatis* strain expressing GFP [20] and we also carried out PI staining of damaged cells for these procedures. However, for the actual separation process no labeling or staining of the cells is required.

With respect to the PI-positive subpopulation, we observed very weak DEP forces acting on these cells throughout the complete frequency spectrum that we probed. Under the buffer conditions used, such forces were not strong enough to induce either pDEP or nDEP. INH targets the biosynthesis of mycolic acids, an essential component of the mycobacterial cell wall, leading to alteration in the cell wall composition and eventual lysis [27], [28], [29], [30]. These results support the hypothesis that physically intact and viable cells, including cells that are phenotypically tolerant to INH, have higher polarizability compared to the surrounding DEP buffer (in this case σ = 500 μS/cm) at frequencies between 1 and 10 MHz, owing to an impermeable plasma membrane and cell wall. In contrast, cells damaged by INH have leaky membrane properties, making the conductivity difference between their cytoplasm and the surrounding DEP buffer negligible.

Once the overall DEP behavior of intact *M. smegmatis* cells was determined, the next step was to determine the frequency at which the pDEP force was the strongest. This was essential since the pDEP force must overcome the fluidic drag acting on intact cells in order to enrich this subpopulation from the flow. Therefore, the stronger the pDEP force is, the higher the velocity of the fluidic flow can be, allowing faster enrichment and high-throughput cell processing. Cell suspensions were loaded into the DEP electrode array as described before and subjected to a 20 Vpp sinusoidal electric field with frequencies between 1 and 10 MHz, as described in detail in the Methods above. In order to quantify the pDEP behavior, time-lapse movies were analyzed by measuring the total intensity in a defined rectangular region,Fig. 2C.The total fluorescence intensity of the region was taken to correspond to the number of trapped cells around the electrodes. While pDEP is induced when using frequencies between 1 and 10 MHz, we found that 7 MHz provided the strongest attraction force to the electrodes in a medium with conductivity of 500 μs/cm (Fig. 3).

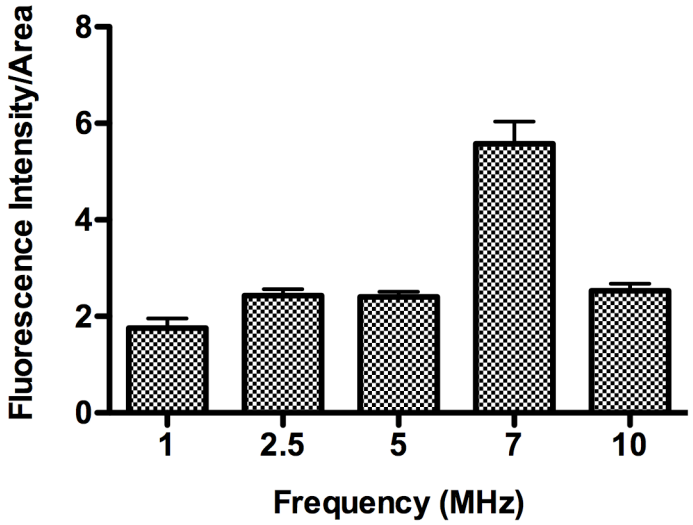

Figure 3. DEP-based purification of INH-treated bacteria. pDEP response of intact GFP-expressing *M. smegmatis* cells scanning the frequencies 1–10 MHz at 20 Vpp. Cells (white) are trapped at regions of high electric field strength around the electrodes (black circles) and visualized by phase-contrast and epifluorescence microscopy. The x-axis shows the scanned frequencies. The y-axis shows fluorescence intensity normalized to area, as indicated in Figure 2C by the rectangular frame. Bars and error bars represent mean values ± SEM of data from three independent experiments.

3.2 Separation of INH-treated bacterial subpopulations using 3D-carbonDEP

After the optimal frequency to induce pDEP on intact cells was determined, an experimental protocol was designed to extract these cells from the flow medium. Here the strategy was to retain the intact cells by pDEP while allowing the drug-damaged cells to flow through, rather than separating populations by shifting streams of targeted cells to specific outlets.

As described in detail in the Methods, the flow rate of sample and DEP buffer in the channel during DEP trapping was 2 µl/min. Flow rates higher than 2 µl/min led to significantly reduced trapping (data not shown). pDEP trapping is expected as long as the DEP force induced on intact cells is stronger than the hydrodynamic drag acting on the particle at such flow rate. As expected, intact cells (GFP-positive, PI-negative) were trapped around the electrodes while damaged cells (GFP-positive, PI-positive) flowed through. The entire experiment, including DEP treatment of the sample and washing and elution of pDEP-trapped cells, should not to exceed 2 hours, an

important criteria to keep the phenotype stable.

The different subpopulations in the eluted fractions were analyzed by flow cytometry in order to assess the efficiency of intact cell enrichment and damaged cell depletion. The results of the enrichment protocol are shown in Fig. 4. Initially, before the application of the electric field, the cell suspension comprised a mixture of intact cells (GFP-positive, PI-negative) and damaged cells (GFP-positive, PI-positive). Following enrichment using the carbon electrodes, and flushing of the damaged cells, the eluted fractions, especially from fraction 5 onwards, were enriched for intact cells, achieving upwards of 99% purity (Fig. 4A).

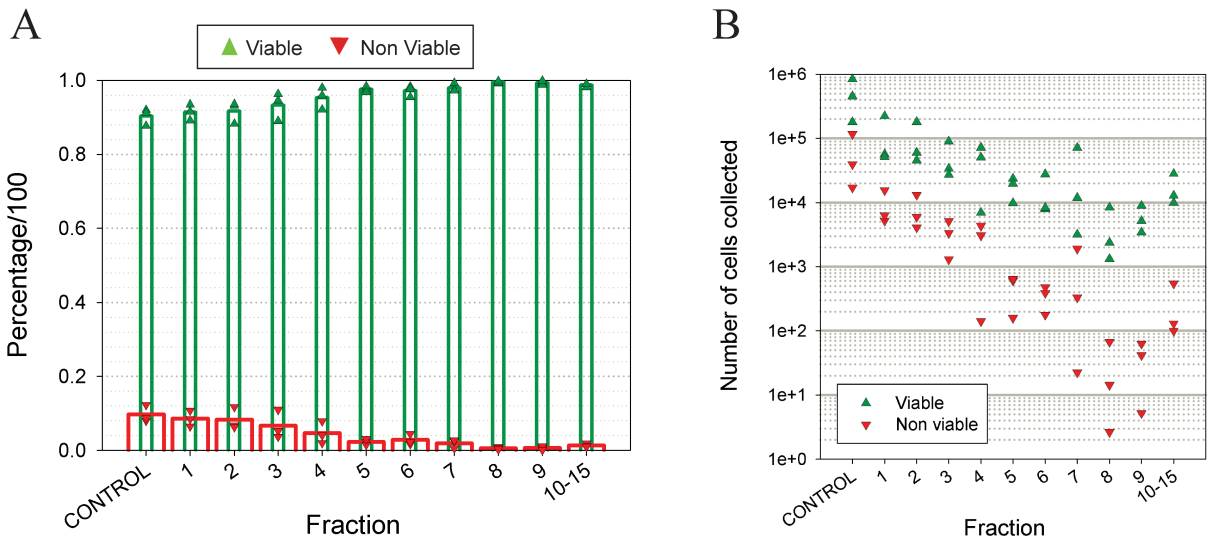

Figure 4. Flow cytometric analysis of composition of cell fractions obtained by DEP-based separation of INH-treated bacteria. A) Normalized percentage of intact versus damaged cells for each cell fraction (y-axis) plotted for each cell fraction (x-axis). The "control" fraction was processed through the system but without application of the electric field. Green bars represent intact cells (GFP-positive, PI-negative); red bars represent damaged cells (GFP-positive, PI-positive). Bars and error bars represent mean values ± SEM of data from three independent experiments. **B)** Intact and damaged cell counts (y-axis) of the fractions (x-axis) recovered from the 3D-carbon DEP chip after DEP-based separation of INH-treated bacteria. The "control" fraction was processed through the system but without application of the electric field. Green triangles represent intact cells (GFP-positive, PI-negative); inverted red triangles represent damaged cells (GFP-positive, PI-positive). Symbols represent data from three independent experiments.

4. Discussion

Recently, the DEP properties of bacteria have been extensively investigated [31-37], especially in the context of drug evaluation [38], antibiotic susceptibility [39], and dormancy [40]. To investigate mechanisms of dormancy or drug-cell interactions in mycobacterial infections such as tuberculosis, the non-pathogenic species *M. smegmatis* is well suited as a model organism. Dielectrophoretic approaches to investigate dormancy in mycobacteria has so far concentrated on the separation of dormant (stationary phase, non-growing) and non-dormant (actively growing) *M. smegmatis* cells [40], and monitoring the resuscitation of dormant *M. smegmatis* in DEP-generated microbial aggregates [41]. However, dormant cells were not naturally pre-existent as a fraction of the overall population in these studies; rather, active, dormant, and dead cell populations were prepared separately and pre-mixed before introduction into the DEP platform, and the conductivity of the surrounding medium and electric field frequency were subsequently fine-tuned for separating these subpopulations.

A recent study on DEP-based characterization of wild type *M. smegmatis* and antibiotic-treated *M. smegmatis* using other antibiotics targeting cell wall integrity, such as ethambutol, yielded similar results to those reported here [32]. Hawkins et al. presented the dielectrophoretic response of wild type *M. smegmatis* and ethambutol-treated *M. smegmatis* cells. Their data confirmed the effect of ethambutol on mycobacterial membrane integrity, as the pDEP response of ethambutol-treated *M. smegmatis* cells is shifted toward higher frequencies [32]. The fact that cells surviving drug treatment experience pDEP suggests that these cells probably have an unaltered cell wall or have incorporated some other modification that allows them to survive cell wall component biosynthesis inhibition.

The advantages of dielectrophoretic separation compared to other cell sorting technologies have been discussed before, particularly when the advantages of carbon 3D electrodes were compared to metal 2D electrodes [18]. CarbonDEP offers simpler and less expensive manufacturing; furthermore, carbon is more electrochemically stable than gold and platinum, has excellent biocompatibility, and is relatively inert to a wide range of chemicals. Since carbon is electrically conductive, the voltage levels needed for DEP experiments are in the order of tens of volts. On the other hand, DEP systems also have some limitations, which may restrict their usage in some diagnostic and clinical applications, such as the need for an electric field, which may disturb the

behavior of the cell, and the fact that low electrically-conductive medium is usually necessary to induce a strong pDEP force, thus limiting the use of physiological media in DEP experiments and requiring buffer optimization.

Flow cytometry was used to quantify the separation efficiency of "intact" and "damaged" cells in this proof-of-concept study because of its advantages of high throughput and rapid readout. We reasoned that traditional CFU-based approaches would be less informative as a readout, because (i) intact and but non-growing subpopulations, such as NGMA cells [4], cannot be enumerated by growth-based assays, (ii) CFU-based assays require 3-4 days' time for outgrowth, allowing the persisters to lose their metastable phenotype, and (iii) the plating procedure, being a retrospective assay, could skew the results because the procedure itself can cause killing on the agar plates [42]. We also attempted to quantify the viability of antibiotic-exposed cells by direct counting of PI-negative and PI-positive cells under the microscope, but this approach proved to be low-throughput and prone to error due to clumping of mycobacterial cells.

The results presented here demonstrate DEP-based enrichment of intact *M. smegmatis* cells from a mixed input population of INH-treated cells comprising about 90% intact cells (PI-negative) and 10% damaged cells (PI-positive). The large fraction of intact cells in the input population is explained by the fortuitous observation that pre-filtration of the INH-treated culture preferentially removes clumps of damaged cells, thus providing a rapid pre-DEP purification step (data not shown). Prior to filtration, the proportions of intact cells and damaged cells are expected to behave similar to the proportions of live cells versus dead cells reported for other experiments with INH [20]. In this study, we focused on INH due to its continued widespread use as a key drug in global tuberculosis control strategies, and because the rate of persistence against INH is relatively high compared to other anti-tuberculosis drugs and drug combinations [43], [44]. DEP-based purification of persister cells could provide a useful tool to shed more light into the mechanisms of persistence under INH exposure. Optimization of the carbonDEP device geometry and the polarization protocol could lead to higher levels of enrichment, if this is deemed necessary when using other antibiotics or in other applications.

Most of the 'omics based approaches for downstream characterization of purified bacterial populations require a sample containing at least 10^5-10^6 targeted cells. As can be seen from Fig. 4B, we were able to recover up to $3X10^4$ intact cells, with up to 99% purity, following the assay protocol demonstrated in this work. Using this setup, serial assays could provide the user with

enough material to perform downstream analysis. Alternatively, current studies are focused on the improvement of device performance in terms of throughput, by increasing the dimensions and number of electrodes in the carbonDEP array.

5. Conclusion

The main purpose of this work was to demonstrate the use of a DEP-based protocol to separate phenotypically different bacterial subpopulations after antibiotic exposure. To the best of our knowledge, this is the first study demonstrating that antibiotic-treated mycobacterial subpopulations can be both enriched and recovered for downstream analysis using a DEP system. This procedure is label-free and separation is based on the intrinsic dielectric properties of cells. The isolation and purification of subpopulations could facilitate the analysis of a low frequency or impure populations using conventional "batch" approaches such as transcriptome and proteome profiling. In this study, efforts were focused on optimizing the method to allow separation of *M. smegmatis* cells based on only small changes in their intrinsic properties, such as membrane integrity, rather than differences in size, shape, or volume. Following antibiotic treatment, intact and damaged cells were separated via DEP; intact cells were then washed and recovered from the device. Enrichment was confirmed by using flow cytometry and purification exceeding 99% was achieved, with recovery of up to $3X10^4$ cells of interest from the device for further analysis.

Acknowledgements

The authors thank Thomas Braschler, Ana Valero, and Katrin Schneider for their assistance in preliminary experiments.

References

1. J. W. Bigger, *Lancet,* 1944, 2, 497-500.
2. N. Dhar, J. D. McKinney, *Curr.Opin.Microbiol.,* 2007, 10, 30-38.
3. M. Fauvart, V. N. De Groote, J. Michiels,*J.Med.Microbiol.,*2011, 60, 699-709.
4. G, Manina, J. D. McKinney, *Curr. Top.Microbiol.Immunol*, 2013, 374,135-161.
5. H. M. Davey, P. Hexley, *Microbiol.,* 2011, 13, 163-171.
6. A. F. Altelaar, J. Munoz, A. J. R. Heck,*Nat. Rev. Genet*., 2013, 14: 35-48.
7. H. Stower, *Nat. Rev. Genet*., 2013, 14, 596-596.
8. R. Hölzel, N. Calander, Z. Chiragwandi, M. Willander, F. F. Bier, *Phys. Rev. Lett*., 2005, 95,

128102-128106.
9. Z. Gagnon, H. C. Chang, *Electrophoresis*, 2005, 26, 3725-3737.
10. I. Peitz, R. vanLeeuwen, *Lab Chip*, 2010, 10, 2944-2951.
11. P. Gascoyne, C. Mahidol, M. Ruchirawat, J. Satayavivad, P. Watcharasit, F. Becker,*Lab Chip,* 2002, 2, 70-75.
12. M. P. Hughes, H. Morgan, F. J. Rixon, *Biochim.Biophys.Acta.*, 2002,1571, 1-8.
13. C. F. Chou, J. O. Tegenfeldt, O. Bakajin, S. S. Chan, E. C. Cox, N. Darnton, T. Duke, R. H. Austin, *Biophys. J.*, 2002, 83, 2170-2179.
14. G. Giraud, R. Pethig, H. Schulze, G. Henihan, J. G. Terry, A. Menachery, I. Ciani, D. Corrigan, C. J. Campbell, A. R. Mount, P. Ghazal, A. J. Walton, J. Crain and T. T. Bachmann,*Biomicrofluidics*, 2011, 5, 024116-024132.
15. R. W.Clarke, S. S. White, D. Zhou, L. Ying, D. Klenerman,*Angewandte.Chemie.*, 2005, 117, 3813-3816.
16. R. W. Clarke, J. D. Piper, L. Ying and D. Klenerman, *Phys. Rev. Lett.*, 2007, 98, 198102-198106.
17. B. H. Lapizco-Encinas, S. Ozuna-Chacón, M. Rito-Palomares,*J.Chromatogr.*A, 2008, 1206, 45-51.
18. R. Martinez-Duarte, P. Renaud, M. J. Madou,*Electrophoresis,* 2011, 32, 2385-2392.
19. Y. Demircan, E. Özgür E, H. Külah,*Electrophoresis,* 2013, 4, 1008-1027.
20. Y. Wakamoto, N. Dhar, R. Chait, K. Schneider, F. Signorino-Gelo, S. Leibler, J. D. McKinney,*Science,*2013, 339, 91-95.
21. T. B. Jones,*IEEE Eng. Med. and Biol.,*03, 22, 33-42.
22. R. Pethig, *Biomicrofluidics*, 2010, 4, 022811-022846.
23. M. C. Jaramillo, E. Torrents, R. Martínez-Duarte, M. J. Madou, A. Juárez, *Electrophoresis*, 2010, 31, 2921-2928.
24. R. Martinez-Duarte, *Electrophoresis*, 2012, 33, 3110-3132.
25. R. Martinez-Duarte, F. Camacho-Alanis, P. Renaud, A. Ros, *Electrophoresis,* 2013, 34, 1113–1122.
26. M. C. Jaramillo, R. Martínez-Duarte, M. Hüttener, P. Renaud, E. Torrents, A. Juarez, *Biosens. Bioelectron,* 2013, 43, 297-303.
27. K. Takayama, L. Wang, H. L. David, *Antimicrob. Agents.Chemother.*, 1972, 2, 29-35.
28. L. Wang, K. Takayama, *Antimicrob. Agents.Chemother.*, 1972, 2, 438-441.
29. G. S. Timmins, V. Deretic, *MolMicrobiol.*, 2006, 62, 1220-1227.
30. C. Vilchèze, J. W. R. Jacobs, *Annu. Rev.Microbiol.*, 2007, 61, 35-50.
31. P. Patel, G. H. Markx, *Enzyme Microb. Tech.*, 2008, 43, 463-470.
32. B. G. Hawkins, C. Huang, S. Arasanipalai, B. J. Kirby, *Anal. Chem.,* 2011, 83, 3507-3515.
33. J. Johari, Y. Hubner, J. C. Hull, J. W. Dale and M. P. Hughes, *Phys. Med. Biol.*, 2003, 48, 193-198.
34. J. Suehiro, R. Hamada, D. Noutomi, M. Shutou, M. Hara,*J.Electrostat,*, 2003, 57, 157-168.
35. J. Suehiro, R. Yatsunami, R. Hamada, M. Hara,*J. Phys. D: Appl. Phys.*, 1999, 32, 2814-2820.

36. M. Castellarnau, A. Errachid, C. Madrid, A. Juarez, J. Samitier, *Biophys. J.*, 2006, 91, 3937-3945.
37. L. Yang, P. Banada, A. K. Bhunia, R. Bashir, *J. Biol. Eng.,* 2008, 2, 6-20.
38. K. F. Hoettges, Y. Hubner, L. M. Broche, S. L. Ogin, G. E. Kass, M. P. Hughes. *Anal.Chem*., 2008, 80, 2063-2068.
39. C. C. Chung, I. F. Cheng, H. M. Chen, H. C. Kan, W. H. Yang, H. C. Chang, *Anal. Chem*., 2012, 84, 3347-3354.
40. K. Zhu,A. S. Kaprelyant, E. G. Salina, and G. H. Markx, *Biomicrofluidics*, 2010, 4, 022809-022820.
41. K. Zhu, A. S. Kaprelyants, E. G. Salina, M. Schuler, G. H. Markx, *Biomicrofluidics*, 2010, 4, 022810-022823.
42. E. Gelman, J. D. McKinney, N. Dhar, *Antimicrob. Agents Chemother*., 2012, 56, 3610-3614.
43. F. Wallace, A. E. Gordon, A. M. Denis,*Int. J.Tuberc. Lung D.,* 31999, 3, S231-S279.
44. D. A. Mitchison, *Handb. Exp. Pharmcol.*, 2012, 211, 87-98.